



## JRA4: REAL-TIME SEISMIC RISK

Andrea BIANCHI<sup>1</sup>, Barbara BORZI<sup>2</sup>, Marta FARAVELLI<sup>3</sup>, Marcus HERRMANN<sup>4</sup>, J. Douglas ZECHAR<sup>5</sup> and Warner MARZOCCHI<sup>6</sup>

### ABSTRACT

In this project we seek to include the effects of progressive damage in estimating damage scenarios and seismic risk. We combine two main research activities: estimating time-varying seismic hazard and modelling vulnerability that includes the effects of the sequences of ground shaking on the buildings.

We have applied time-varying seismic risk estimation to two case studies, the first one inspired by a hypothetical repeat of the 1356 M6.6 earthquake in Basel, Switzerland, and the second one relevant to a hypothetical repeat of the M6.9 earthquake in Calabria, Italy.

For the Basel scenario, we consider an entire sequence of earthquakes that was simulated for the SEISMO-12 disaster exercise in Switzerland. This sequence comprises the events that lead to time-varying hazard, and thus time-varying risk. We use a statistical seismicity model to generate short-term forecasts of seismicity rates and transform these to forecasts of hazard, i.e., the probability of exceeding specific shaking intensities. We apply these hazard forecasts to a building stock model of the potentially-affected settlements surrounding Basel and estimate the resultant seismic risk in terms of human losses. We can generate these forecasts at arbitrary time intervals (regular or irregular) and have developed tools to visualize the results in a number of ways.

For the scenario in Calabria, more than 1500 events above magnitude 2 with a stochastic point process model have been simulated: these events are taken to represent a six-month long sequence, including a strong aftershock. As in Basel, we used a statistical model to estimate the number of events in the following days: for each of the first fifteen days after the M6.9, a new forecast for the next month is produced. The forecasts is given as probabilistic displacement response spectra. The method adopted for this case study is an upgrade of the method SP-BELA (Simplified Pushover-Based Earthquake Loss Assessment) (Borzi et al. 2008a, 2008b). In such a method, the seismic building performance is described by the capacity curve. To account for progressive damage, the capacity curve is updated as the sequence proceeds. The SP-BELA routine has been modified to assess the progressive damage of buildings during a seismic sequence, assuming that both the simulated spectra of ground motion and the actual spectra derived for a real aftershock will be available.

---

<sup>1</sup> Eucentre, European Centre of Training and Research in Earthquake Engineering, Pavia, andrea.bianchi@eucentre.it

<sup>2</sup> Eucentre, European Centre of Training and Research in Earthquake Engineering, Pavia, barbara.borzi@eucentre.it

<sup>3</sup> Eucentre, European Centre of Training and Research in Earthquake Engineering, Pavia, marta.faravelli@eucentre.it

<sup>4</sup> Swiss Seismological Service, Zürich, marcus.herrmann@sed.ethz.ch

<sup>5</sup> Swiss Seismological Service, Zürich, jeremy.zechar@sed.ethz.ch

<sup>6</sup> Istituto Nazionale di Geofisica e Vulcanologia, Rome, warner.marzocchi@ingv.it

## INTRODUCTION

Seismic vulnerability is a measure of how prone a building is to damage for a given severity of the ground shaking. The aim of much of the research work dedicated to this subject is to give a mathematical formulation to the vulnerability.

The two most largely utilised formulations to describe the vulnerability are damage probability matrices (DPMs) and vulnerability curves. A vulnerability curve describes the conditional probability of exceeding a certain level of damage in terms of the selected intensity of the ground motion. The same probability in discrete terms is a component of a damage probability matrix. The conditional probability is expressed with Eq.1:

$$P_{ik} = P[D \geq d_i | S = s_k] \quad (1)$$

where  $P_{ik}$  is the probability that the damage level  $d_i$  will be achieved or exceeded for a ground motion severity  $s_k$  and  $D$  and  $S$  are the variables representing the damage and the severity of the input motion, respectively.

In the technical literature, DPMs have been produced when vulnerability studies are based on observations: data from post-earthquake surveys are treated probabilistically to identify the conditional probability of damage. On the other hand, fragility curves are calculated when the vulnerability studies are mechanics-based, i.e. the seismic behaviour of structures is modelled. The model can be more or less simplified as a function of the level of knowledge of the building stock.

In this paper we consider two case studies:

- in the Basel case study, the vulnerability of the building stock is described by DPMs which contain the distribution of damage grades among the vulnerability classes as a function of intensity—essentially discretized fragility functions stated in a different way. DPMs are modeled from vulnerability indices using the European Macroseismic Method (EMM, Giovinazzi and Lagomarsino 2004)—a simplified vulnerability method based on linguistic (qualitative) definitions in EMS-98 (Grünthal 1998). EMM has not been designed for including progressive damage since corresponding data are scarce. But we apply empirical relations that translate damage states to casualty degrees, which enables us to estimate short-term casualties, e.g., the individual risk of dying within the next day. Fatalities mostly occur for collapsed buildings (damage grade 5);
- in the Calabria case study, the vulnerability is modeled through the SP-BELA method. This method has been originally published in the technical literature to define fragility curves of reinforced concrete (Borzi et al. 2008a) and masonry structures (Borzi et al. 2008b). To account for progressive damage acting directly on building capacity, the building capacity is kept separate from the demand imposed by the ground shaking.

This paper describes the aforementioned case studies, highlighting how we have extended the two adopted methods to account for progressive damage and how we estimate seismic risk based on time-varying hazard.

## BASEL CASE STUDY

To forecast the seismic risk, i.e., the possible consequences that future earthquakes could have on the buildings or the population, we need to connect all the potential losses with the probability that these losses could occur. Potential losses are a function of shaking level; in turn, the probability of reaching a shaking level is expressed by the seismic hazard and typically varies in time.

Following this principle—once aware of the potential (time-invariant) losses—we forecast the seismic hazard at various shaking levels to assess the time-varying risk in terms of expected building damage states or fatalities.

We used relatively high-resolution settlement data in our analysis: Baisch et al. (2009) published the population and building inventory for each of the 19 districts of Basel and 60 surrounding municipalities. The building data contains residential units distributed in Risk-UE

building classes with redefined vulnerability values to account for specific building parameters in the Basel region. To make use of this classification, we converted the Risk-UE typology to EMS vulnerability classes. Therefore, we compared the most probable vulnerability values and assigned the matching EMS class (see Fig.1). Because the distribution of people among the building classes is not given, we make the simplifying assumption that it matches the distribution of building classes.

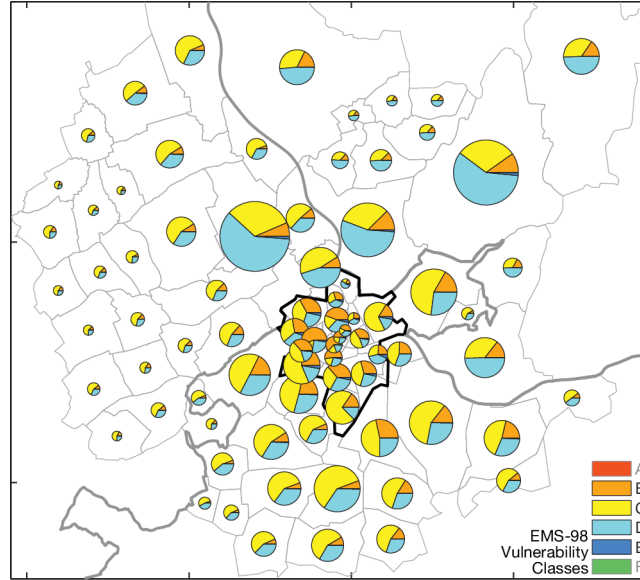


Figure 1. Map-view of processed building inventory information for all 79 locales: we converted the original data set to EMS-98 vulnerability classes to serve as input for the loss estimation. The map reveals varying building vulnerability (with only classes B-E present). The city of Basel is enclosed by the thicker black boundary

To estimate the potential losses at a given shaking intensity, we adopt the loss estimation procedure of *QLARM* (Trendafiloski and Wyss 2009), a tool used to quantify losses after disastrous events, or to model deterministic scenarios. *QLARM* models the building damage using the buildings' vulnerability,  $V_j$ , to ground shaking,  $I_k$ , and then applies empirical relations,  $M$ , to translate damage states,  $D_n$ , to fatality estimates,  $F(I)$ , (Eq.2):

$$F(I) = \left( \sum_{n=0}^5 \sum_{j=A}^F Pr(C_5 \square D_n, M) Pr(D_n \square V_j) Pr(V_j \square I) \right) \square N \quad (2)$$

with  $C_5$  being the fraction of people dying and  $N$  the population number.

Based on information of the continuous seismic activity, an earthquake occurrence model produces a seismicity rate forecasts for any future period. Subsequently, a ground motion model converts the rate forecast into probabilities of exceeding distinct shaking levels, i.e., EMS-98 intensities (Grünthal 1998), and we obtain a probabilistic hazard forecast (Fig.2). With the loss estimation and the short-term hazard issued for the same shaking levels, we construct so-called loss exceedance curves (Crowley and Bommer 2006).

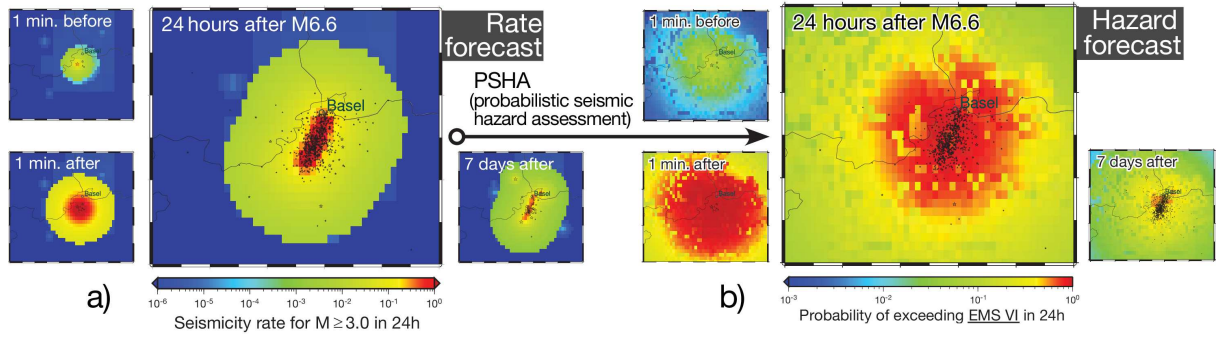


Figure 2. 24-hour forecasts for the Basel region using earthquake data available at the specified time. **a)** Rate forecasts, showing the number of earthquakes above magnitude three that STEP forecasts in each bin over the next 24-hour period. The model estimated a fault after 100 aftershocks (not illustrated); 598 aftershocks occurred 24 hours after the M6.6 (large image). **b)** Short-term hazard forecasts. We use PSHA (probabilistic seismic hazard assessment) to convert the forecast rates into the probability of exceeding various EMS intensities within the next 24 hours. EMS VI was chosen as an example; the scattering results from site amplification data

The loss information shown in Fig.3 was derived from loss exceedance curves. Loss exceedance curves allow risk statements in various terms: for instance, the integral of each curve equals the expected number of fatalities,  $E[f]$ , in the respective municipality for the next day. Furthermore, dividing  $E[f]$  by the respective district population yields the probability of an individual dying,  $P_{indv}$ , during this period. We constructed a total loss exceedance curve that represents the regional view of risk by convolving the loss curves for each locale. Since we separated the locales of the city of Basel from the surrounding region, we see in Fig.3 that an individual is at higher risk in the urban area than in the rural area (twice as high). Although only 30 % of the population in the region lives in the city of Basel, we calculated that this subregion contributes to almost half of the losses (in terms of expected fatalities). This observation is likely caused by the following facts: first, the ratio of older masonry buildings (and thus higher vulnerability) is higher in the city than in the rural region; secondly, the city districts are, on average, more proximate to the estimated fault zone.

One minute before the mainshock, the sum of  $E[f]$  among all locales is two fatalities and the mean of  $P_{indv}$  is about  $4 \cdot 10^{-6}$  (Fig.3). One minute after the M6.6, the values are 205 fatalities and  $4 \cdot 10^{-4}$  (0.04 %), respectively.

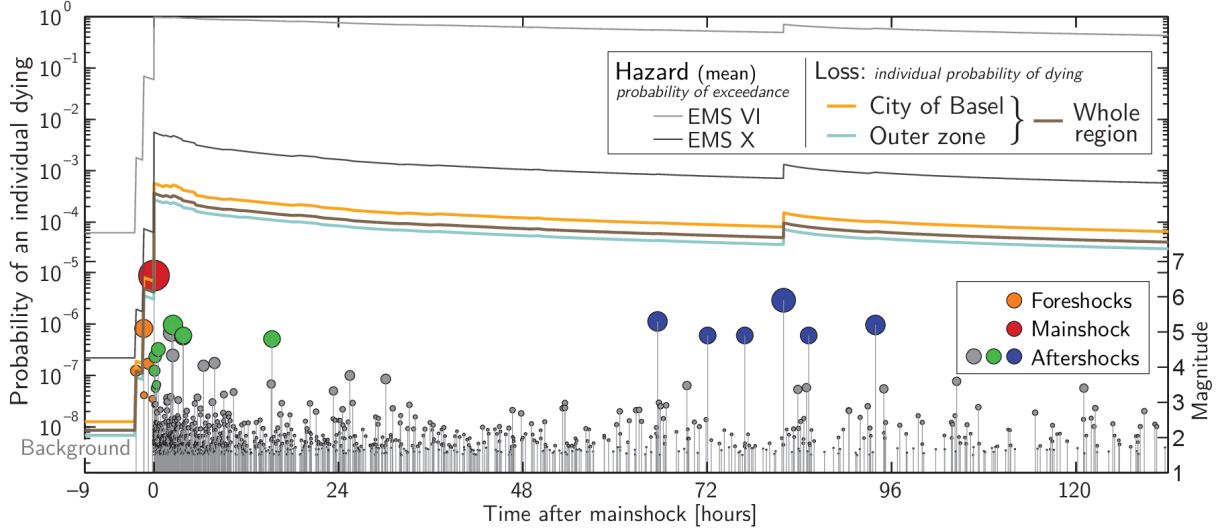


Figure 3. Time-varying probability of hazard and loss before and after the M6.6 event using information available at that time (retrospective). The loss curves indicate the probability that any inhabitant will die in the next 24 hours, separated for the city of Basel (orange), the surrounding region (blue), and the whole region (brown). The hazard curves denote the average probability of exceeding shaking intensity EMS VI (light gray) and EMS X (dark gray) in the whole locality area. The loss and hazard forecasts were issued each hour and apply to the following 24 hours. To track the seismicity during this time, stems at the bottom represent earthquakes

Fig.4 demonstrates an alternative risk statement using a single value from the loss exceedance curve of each locale: it maps the number of fatalities to be exceeded for a fixed exceedance probability. These values are of less practical use, but deliver a spatial and relative impression of the risk.

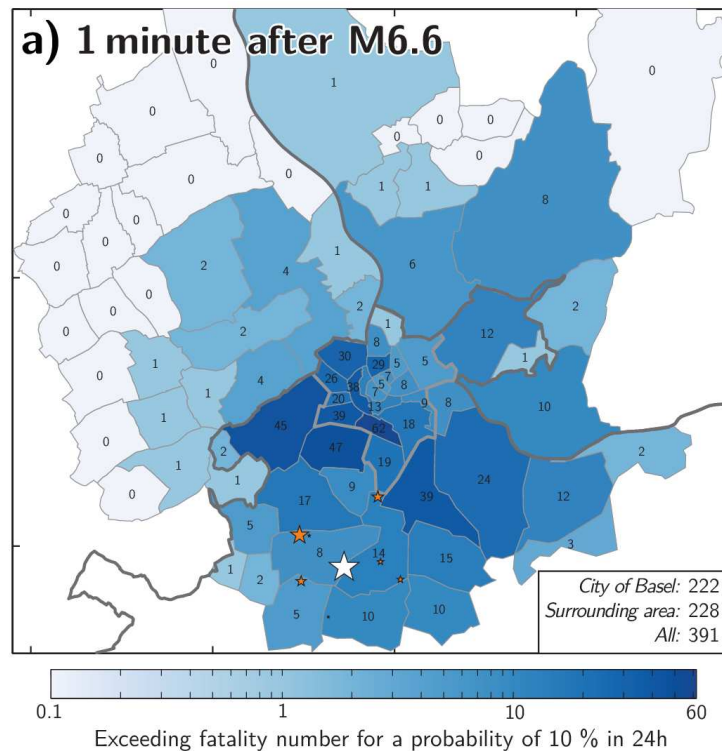


Figure 4. Spatial 24-hour time-varying loss forecast for each locale one minute after the M6.6 (white star). The mapped fatality number will not be exceeded by a chance of 90 % in 24 hours; the values in the lower right results from treating corresponding locales as one unit (which is not the sum)

## CALABRIA CASE STUDY

Since SP-BELA describes the structural performance through a pushover curve, accounting for progressive damage requires to modify pushover curve parameters like initial stiffness, base shear resistance and displacement capacity.

This approach was followed by FEMA (Federal Emergency Management Agency) research groups that had, as major inspiration, to provide professionals with practical guidance on how to take into account pre-existing damage of a structure. In 1998, two documents were published on the evaluation of earthquake-damaged concrete and masonry wall buildings: a basic procedure manual (FEMA306, 1998) and a technical resource manual (FEMA307, 1998).

For the Calabria case study, the SP-BELA method defines the building capacity without computing the fragility curves. This choice has two main advantages for the applications within the NERA project. The first is that the effects of the frequency content of the ground shaking can be explicitly taken into account when evaluating the probability of reaching or exceeding a damage limit condition through a comparison between displacement demand and capacity. An alternative could be to compute the fragility curve as a function of a ground shaking parameter (e.g. PGA) anchoring a spectral shape to each point of the abscise of the curve. Such a shape does not match the one corresponding to the earthquake that shall be considered to calculate the seismic risk. The second advantage is that the effect of progressive damage can be computed by directly modifying the capacity curve. The SP-BELA routine has been updated to assess the progressive damage of buildings during a seismic sequence, assuming that both simulated data of ground motion and actual spectra derived for a

real aftershock will be available. The flow chart of the procedure is shown in Fig.5. Initially, the pushover curves of the undamaged building are computed and two different paths can be followed:

- if the simulated hazard is used as an input, then the seismic risk is calculated but the pushover curves are not updated since a further shaking did not really occur;
- if the ground shaking scenario is real, i.e., a real aftershock has occurred, then the damage scenario is computed and, as a function of the performance point reached by each building, the properties of the pushover curve are updated.

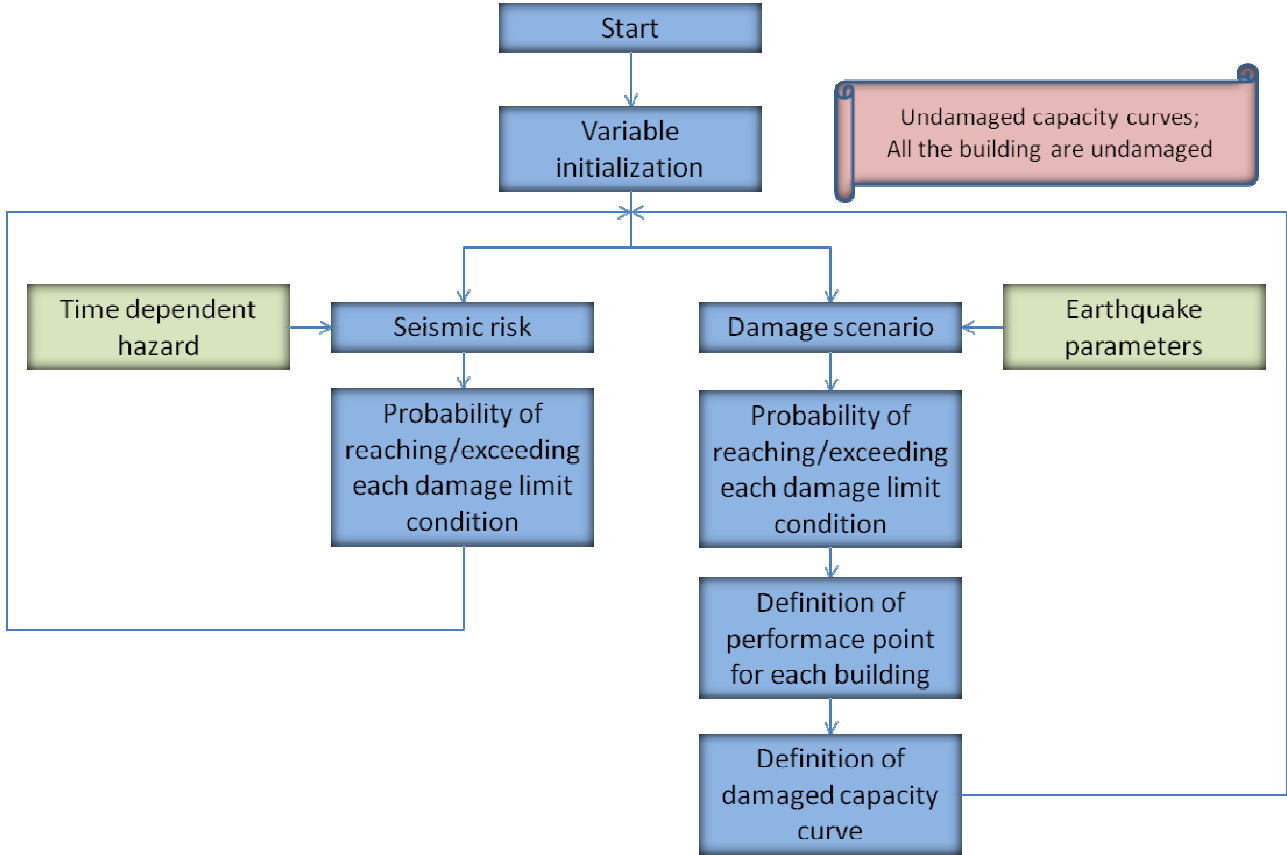


Figure 5. Workflow of the procedure to account for progressive damage

The flow chart shown in Fig.5 has been implemented in a WebGIS platform, as a support tool to compute time-varying seismic risk and damage scenario accounting for progressive damage. A screenshot of the platform is shown in Fig.6.

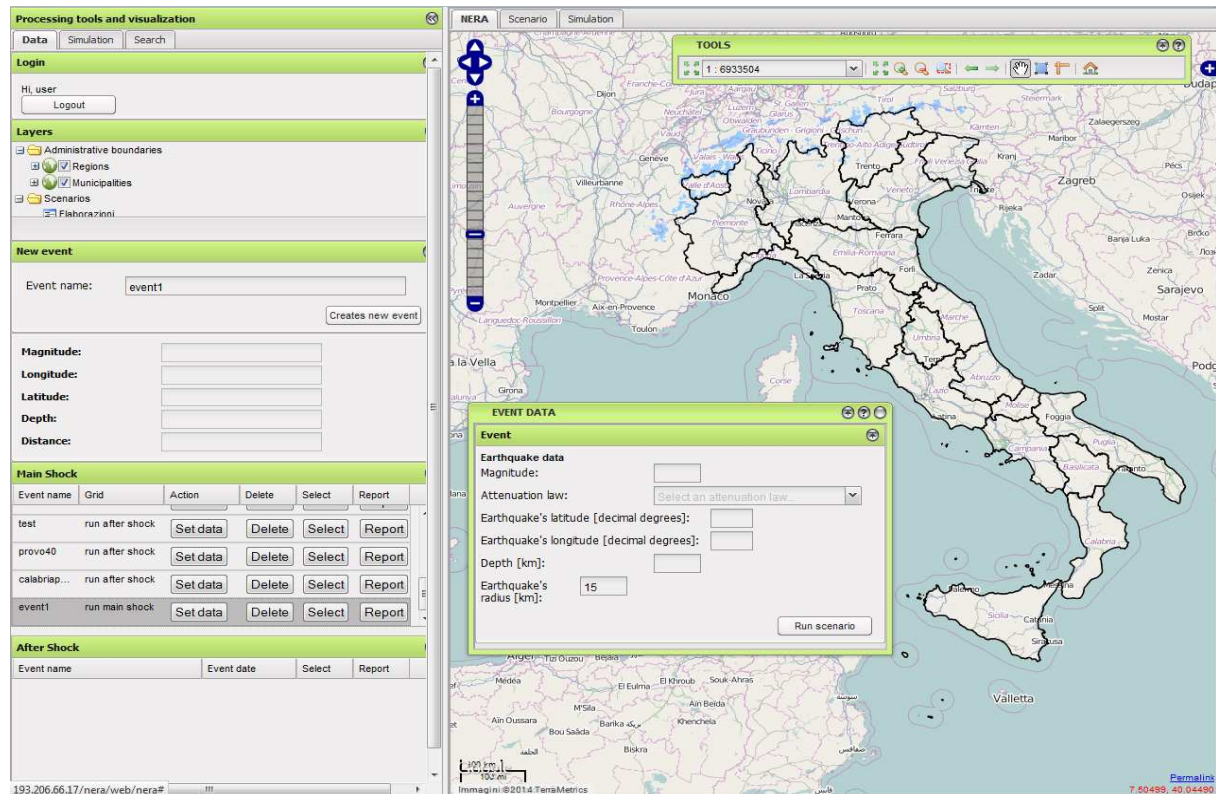


Figure 6. Screenshot of the WebGIS platform

For the Calabria case study, we have simulated the occurrence of a mainshock similar to which occurred in Calabria region (Southern Italy) at 1783—with a moment magnitude  $M_w$  of 6.9, located at  $16.47^\circ\text{E}$ ,  $38.78^\circ\text{N}$  in 10 km depth (Fig.7). Then we have simulated the sequence that follows the occurrence of the main event in terms of displacement spectra. In particular, the results shown in this paper refers to what happened in the first 3 days after the mainshock. On the fourth day, we hypothesized the occurrence of an aftershock of local magnitude 6.0 at  $16.565^\circ\text{E}$ ,  $38.932^\circ\text{N}$  with a focal depth of 10 km (Fig.8). In reality, this aftershock has happened on the eighth day after the main event. In our analysis, we have used a radius of 30 km, so Fig.9 includes the number of buildings reaching or exceeding the five damage levels for those municipalities that are less than 30 km from both the epicenters.

We have considered five damage levels from light damage to collapse. These damage levels are the same as in the EMS-98 scale (Grünthal 1998). The SP-BELA method evaluates the building capacity in terms of displacement and compares it with the displacement imposed by the earthquake with reference to the limit states identified numerically. To create damage scenarios, we have identified a relationship between the limit states and the damage level using the observed damage data considered in the study of Lagomarsino and Giovinazzi (2006).

In order to account for progressive damage, we use FEMA coefficients (FEMA307, 1998) for bare frames, frames with infill wall, and masonry panels. The coefficients applied to the pushover curves are linearly interpolated between light damage and collapse limit conditions as a function of the performance point corresponding to the previous shaking. The pushover curve is not modified if the building does not exceed the light damage limit condition.

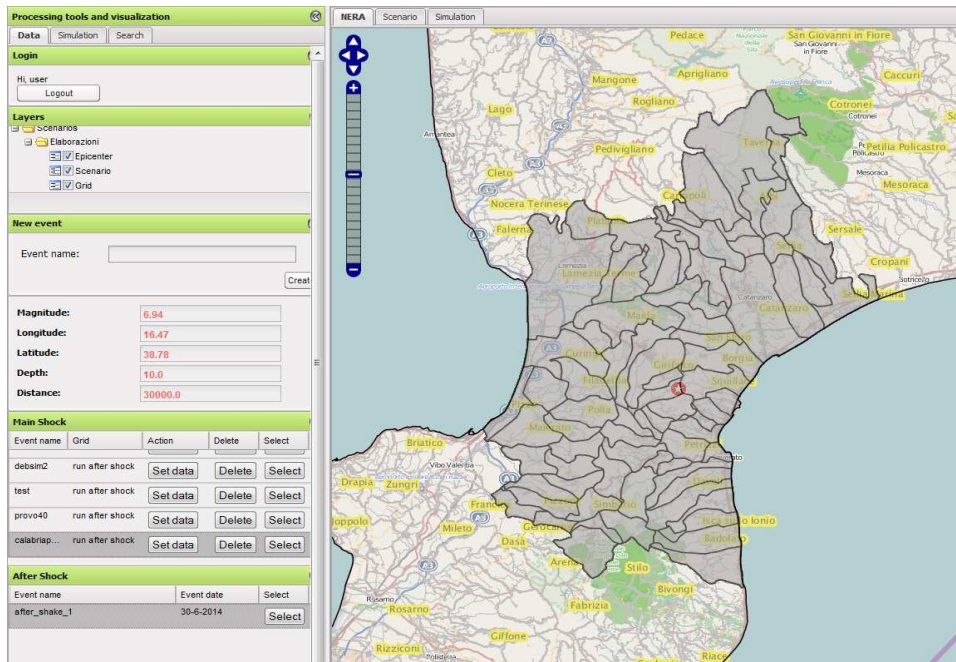


Figure 7. Mainshock in the WebGIS platform

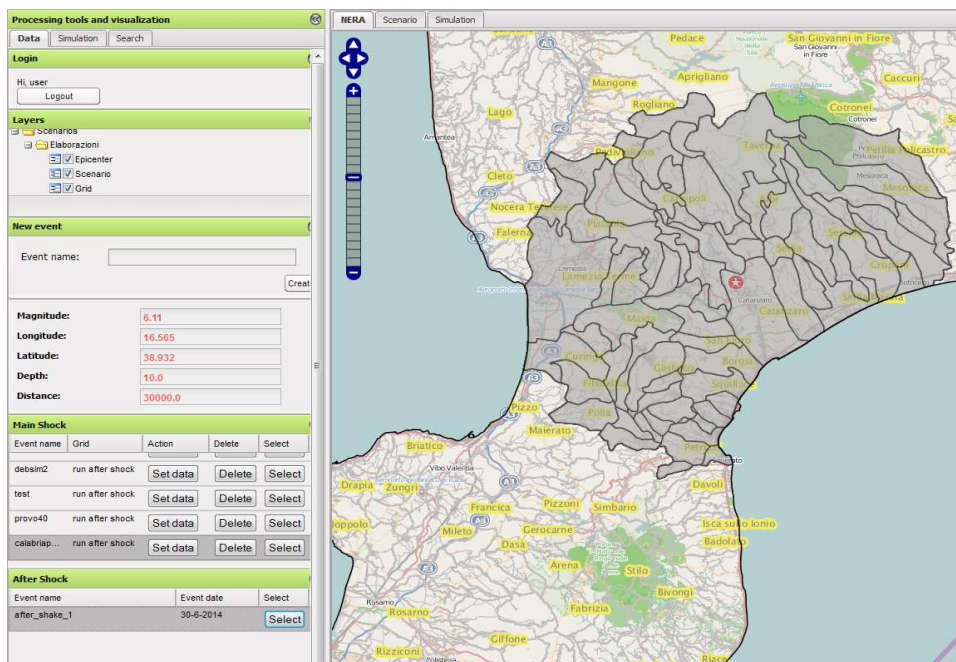


Figure 8. Aftershock in the WebGIS platform

From Fig.9 we can see that during the simulations and the aftershock, the number of buildings reaching or exceeding the five damage levels is greater than after the mainshock. We expected this behavior because of the damage cumulation: the occurrence of a real event, mainshock or aftershock, changes the building capacity. So if at the beginning the capacity is represented by pushover curves at time zero, after the mainshock the curves are modified to take account for the building damage. The damage calculations for the simulations are then based on these changed capacity curves. Thus, the damage simulation for day  $x+1$  and the simulations of the following days always use the same pushover curves, because it is the only event that really happened. The simulations do not change the capacity curve because the displacements did not really happen. Since the spectral displacement of the simulations decreases as time goes from the mainshock, the number of buildings reaching or exceeding the damage levels decreases from simulation 1 to simulation 3.

When the aftershock happens, the capacity should be represented by the modified curves, ie those which take into account the cumulative damage, and not by the curves at time zero. Since the ground shaking really occurred, the capacity curves are further updated. Fig.9 shows that the number of buildings reaching or exceeding the five damage levels after the aftershock is correctly greater than after the mainshock.

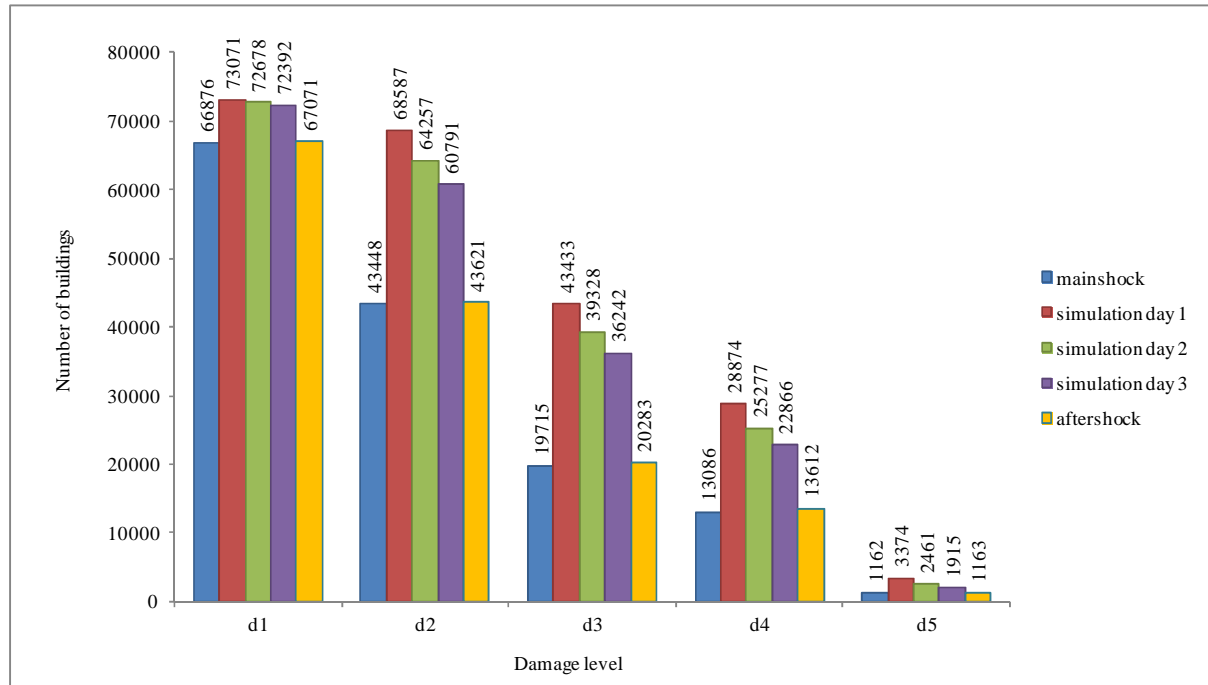


Figure 9. Number of buildings reaching or exceeding a certain damage level, considering all municipalities that are less than 30 km from both epicenters

The maps in Fig. 10 and Fig.11 show the percentage of buildings reaching or exceeding damage level 1 and 3 in each municipality, respectively. We can see that the percentage of damaged buildings increases particularly near the epicenter of the aftershock.

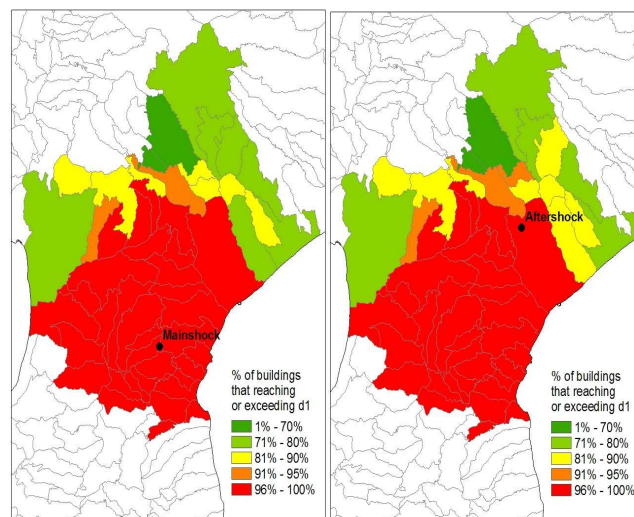


Figure 10. Percentage of buildings reaching or exceeding the damage level 1 in each municipality

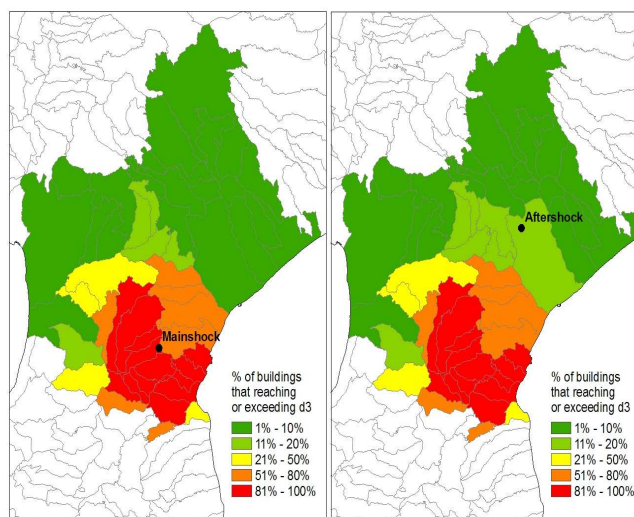


Figure 11. Percentage of buildings reaching or exceeding the damage level 3 in each municipality

## CONCLUSIONS

With our work, we contribute to forecast short-term seismic risk during an aftershock sequence. This ability is the first step of personal decision-making and raises public risk awareness. Worthy of note, almost always the still limited forecasting skill of the available short-term forecasting models does not allow decision makers to plan any rationale strong risk mitigation action, such as evacuation of areas interested by seismic sequences. In fact, using a first order cost benefit analysis, Van Stiphout et al. (2010) showed that the costs of evacuations would not be justified by the small probabilities that are usually obtained by the available short-term forecasting models. Nonetheless, it is clear that many other more “light” mitigation actions could be made, for instance, assisting rescue teams to minimize their exposure inside vulnerable buildings.

In this first analysis, we still neglected many uncertainties, based on simplified assumptions (e. g., that all residents would behave the same) or limited data availability (e. g., no individual building response to shaking), and these uncertainties may not be reduced substantially in the near future. Of course, our loss forecasting approach follows a modular approach and we depend on the current state of knowledge; elements can be exchanged and improved once new insights become available.

## REFERENCES

- Baisch S, Carbon D, Dannwolf US, Delacou B, Devaux M, Dunand F, Jung R, Koller M, Martin C, Sartori M, Secanell R and Vörös R (2009) SERIANEX - Deep Heat Mining Basel, Technical report
- Borzi B, Pinho R, Crowley H (2008a) “Simplified Pushover-Based Vulnerability Analysis for Large Scale Assessment of RC Buildings,” *Engineering Structures*, 30(3): 804-820
- Borzi B, Crowley H, Pinho R (2008b) “Simplified Pushover-Based Earthquake Loss Assessment (SP-BELA) Method for Masonry Buildings,” *International Journal of Architectural Heritage*, 2(4): 353-376
- Crowley H and Bommer JJ (2006) “Modelling Seismic Hazard in Earthquake Loss Models with Spatially Distributed Exposure,” *Bulletin of Earthquake Engineering*, 4(3), 249-273
- Federal Emergency Management Agency 306 (1998) Evaluation of Earthquake Damaged Concrete and Masonry Wall Buildings, Basic Procedures Manual, Washington DC
- Federal Emergency Management Agency 307 (1998) Evaluation of Earthquake Damaged Concrete and Masonry Wall Buildings, Technical Resources, Washington DC
- Giovinazzi S and Lagomarsino S (2004) “A macroseismic method for the vulnerability assessment of buildings,” *Proc. of 13th World Conference on Earthquake Engineering*, Paper No. 896, Vancouver, Canada
- Grünthal G (1998) European Macroseismic Scale 1998, European Seismological Commission, Luxembourg
- Lagomarsino S and Giovinazzi S (2006) “Macroseismic and mechanical models for the vulnerability and damage assessment of current buildings,” *Bulletin of Earthquake Engineering*, 4, 415-443

- Trendafiloski G and Wyss M (2009) "Loss estimation module in the second generation software QLARM," *Second International Workshop on Disaster Casualties*, 15-16 June, University of Cambridge, UK, Cambridge
- Van Stiphout T, Wiemer S and Marzocchi W (2010) "Are short-term evacuations warranted? Case of the 2009 L'Aquila earthquake," *Geophysical Research Letters*, 37(6)